

Eaglet property, southeastern British Columbia: Re-Os geochronology, sulphur isotopes, and thermobarometry



Z.D. Hora^{1, a}, H. Stein², K. Žák³, and P. Dobeš⁴

¹British Columbia Geological Survey (retired)

²AIRE Program, Colorado State University, Fort Collins, USA

³Institute of Geology of the Czech Academy of Sciences, Prague, Czech Republic

⁴Czech Geological Survey, Prague, Czech Republic

^acorresponding author: zdhora@telus.net

Recommended citation: Hora, Z.D., Stein, H., Žák, K., and Dobeš, P., 2018. Eaglet property, southeastern British Columbia: Re-Os geochronology, sulphur isotopes, and thermobarometry. In: Geological Fieldwork 2017, British Columbia Ministry of Energy, Mines and Petroleum Resources, British Columbia Geological Survey Paper 2018-1, pp. 157-166.

Abstract

New Re-Os age data from three molybdenite samples collected at the Eaglet property in southeastern British Columbia yielded model ages of 200.3, 233.8 and 251.6 Ma, but the significance of these multiple ages remains unclear. Sulphur values of $\delta^{34}\text{S}$ +6.00 to +12.91‰ for celestite are outside the range of published values for sulphates of marine origin and indicate some other crustal source of sulphate. Galena intergrown with celestite shows an overlapping $\delta^{34}\text{S}$ of +12.07‰, but pyrite displays much lower $\delta^{34}\text{S}$ values: +0.99 to -4.84‰. With $\delta^{34}\text{S}$ restricted to -3.93 to -5.04‰, molybdenite suggests a single homogeneous sulphur source, in spite of the three significantly different model ages. Fluid inclusions in fluorite samples display varied fluid types corresponding to three types of fluorite identified macroscopically. This is consistent with the idea of multiphase mineralization described for this deposit in previous reports. The minimum trapping pressure, constrained by temperature and composition, is 2.1 to 2.6 Kb.

Keywords: Eaglet deposit, MINFILE 093A 046, fluorite, celestite, molybdenite, sulphur isotopes, Re-Os geochronology, fluid inclusion microthermobarometry

1. Introduction

The Eaglet property (Fig. 1; MINFILE 093A 046) is a fluorite deposit with a reported resource of 24 Mt averaging 11.5% CaF_2 (Ball and Boggaram, 1985; NI 43-101 noncompliant). Hora et al. (2008, 2010) described the exploration history, petrography, and mineralogy of the deposit and concluded that mineralization was the product of two hydrothermal events: introduction of sulphide minerals with some fluorite into fractured, K-feldspar altered host rock, followed by cataclasis and main fluorite and celestite deposition. A pilot sulphur isotopic study (Hora et al., 2010) analyzed six sulphate samples (celestite, $\delta^{34}\text{S}$ +6.00 to +12.91‰) and two sulphide samples (molybdenite and pyrite, both with $\delta^{34}\text{S}$ between -4.81 and +4.84‰). The sulphur isotope results were explained by either two independent hydrothermal events that tapped different crustal sulphur sources for sulphate and sulphide, or that high-temperature isotope exchange occurred between oxidized and reduced sulphur (Hora et al., 2010).

In this paper, we test the idea of superimposed mineralization pulses at Eaglet using Re-Os age determinations of molybdenite. We also expand the set of $\delta^{34}\text{S}$ determinations to a wider variety of sulphide minerals, and present composition and trapping-temperature data from fluid inclusions in fluorite to examine the possibility of high-temperature isotope exchange.

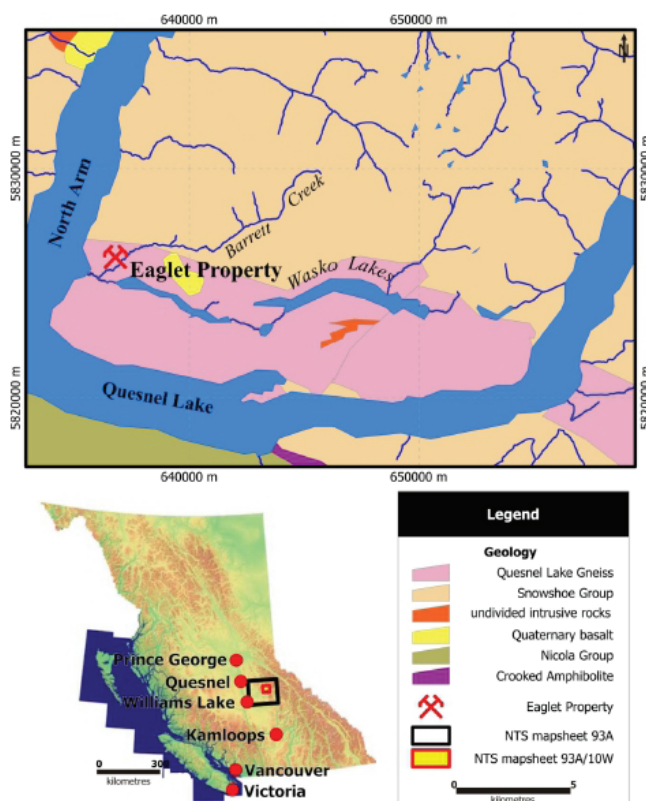


Fig. 1. Location of the study area (UTM Zone 10).

2. Regional geology

The Eaglet deposit is in the pericratonic Kootenay terrane near its border with the accreted Intermontaine superterrane. It is hosted by granitic rocks of the Quesnel Lake gneiss (Early Mississippian) which is part of the Barkerville subterrane. Orthogneiss compositions range from diorite to granite to syenite. U-Pb zircon geochronology indicates an age between 375 and 335 Ma (Ferri et al., 1999). Eaglet mineralization is in the East Quesnel Lake gneiss subunit. This subunit displays I-type characteristics with some assimilation of continental material. Although most geochemical characteristics of the East Quesnel Lake gneiss point to arc magmatism, its origins are not well understood. Ferri et al. (1999) considered that the gneiss is a relic of back-arc spreading during the Late Devonian to Early Mississippian along the western edge of ancestral North America. In this same area, rocks of oceanic character were thrust over the western margin of the Kootenay terrane during Mesozoic collision. Kootenay terrane rocks were metamorphosed from greenschist to amphibolite grade (see Ferri and Schiarizza, 2006 for details).

3. Property history

A summary of the property history can be found in MINFILE (093A 046) and Hora et al. (2008). From its discovery in 1946 until about 1980, Eaglet was considered only as a fluorite resource with silver as a potential byproduct and all samples were analyzed for fluorite only. In 1980, after Placer Development Ltd. examined the property, at that time under active exploration by Eaglet Mines Ltd., a bulk sample with visible molybdenite collected by Eaglet Mines Ltd. from the East Drift area of Adit 2 (Fig. 3) was tested for commercial Mo concentration. In 1985 the property was abandoned. Freeport Resources Inc. took over the property in 1994 and reanalyzed approximately 900 duplicate pulp samples from previous drilling and wall sampling of Adit 2 that had been stored on site by the previous owner (Hora, 2005). Analysis was by inductively coupled plasma mass spectrometry (ICP-MS), reporting either 31 or 34 elements. Results showed that Mo mineralization is more widespread than previously appreciated (Figs. 2, 3). The possibility of deep porphyry mineralization merited further investigation and provided the impetus for the present study.

4. Mineralization

The Eaglet Property, generally considered a fluorite deposit, was originally described as a stockwork of veins, pods, and irregular masses of fluorite-quartz-celestite containing minor Pb, Zn and Mo sulphides (McCammon, 1965). Calcite, pyrite, dickite, and allanite were also listed in the original description. Mineralogical and sulphur isotopic work on samples from drill core and dumps at Adits 1 and 2 (Fig. 2) were carried out by Hora et al. (2008, 2010).

The host rocks are commonly so heavily altered and recrystallized that their gneissic fabric is obscured, and the intensity of feldspar alteration makes distinguishing original

rock types uncertain. Hora et al. (2008, 2010) identified an alteration sequence of widespread albitization followed by K-feldspar alteration, with Nb, Th, Ti and REE mineralization including pyrochlore, REE carbonate (bastnesite?), thorite, and titanbetafite, none of which had been reported previously. XRD analysis revealed fluorapophyllite, also previously unknown. The Nb, Th, Ti and REE minerals exhibit extensive replacement reactions along their contacts, with silicification, albitization and then K-feldspar alteration products, and may have predated the albite-K feldspar alteration (Hora et al., 2010). Following K-feldspar alteration, introduction of some sulphide minerals (MoS_2 , FeS_2) may have occurred, before the oldest generation of fluorite. A period of cataclasis ensued, followed by carbonate alteration and addition of multiple generations of fluorite. Celestite is the last major addition to vein development. Low-temperature hydrothermal alteration superimposed on the mineralized zones introduced quartz, siderite, calcite, zeolite and clay minerals of the kaolinite group (Hora et al., 2008).

Molybdenite is common as a randomly distributed accessory mineral. It can be found along slickenside and gneissosity planes as groups of flakes (Figure 17 in Hora et al., 2008). Molybdenite also occurs as disseminated grains in quartz veinlets (sample MD-1040) and as grains in crosscutting veinlets of fluorite (samples MD 1311 and 1312). Approximately 25% of samples from 13 drill cores from 1983 exploration have Mo concentration ranging from 10s of ppm to 270 ppm (Fig. 2). More than 15% of 562 samples collected from the walls and roof of Adit 2 have between 100 ppm and 1143 ppm Mo (Fig. 3).

Celestite is the latest major hydrothermal component of mineralization. Locally in Adit 2, contents of celestite and fluorite are about equal. Celestite commonly replaces most other minerals (feldspar, quartz, calcite, and fluorite). Pyrite forms isolated crystals with molybdenite in quartz and fluorite but is less common. Sphalerite and galena are rare and spatially associated with calcite. Lead and zinc are usually elevated in the same samples, mainly in 10s of ppm and, locally, in the 100s of ppm (Hora, 2005). Quartz is common as veinlets and cement. Some veinlets contain local disseminated flakes of molybdenite and rare pyrite crystals.

5. Re-Os geochronology

The rhenium-osmium (Re-Os) chronometer is considered a reliable method for dating mineralization, particularly for molybdenite, which can be elevated in Re because it substitutes for Mo in the MoS_2 mineral structure. The Re-Os clock in molybdenite has been shown to withstand intense deformation and high-grade thermal metamorphism (e.g., Stein et al., 2001).

Two sets of samples were used for our laboratory studies. The first was selected from samples collected during a property visit in 2007. They were mainly collected from the dump below Adit 2 (sample prefix QLA) and the core storage facility (sample prefix QLC). Because of concerns of sample weathering, we also used a second set of samples, which was collected in 1984 from a 60 m-long, highly mineralized section of the East Drift

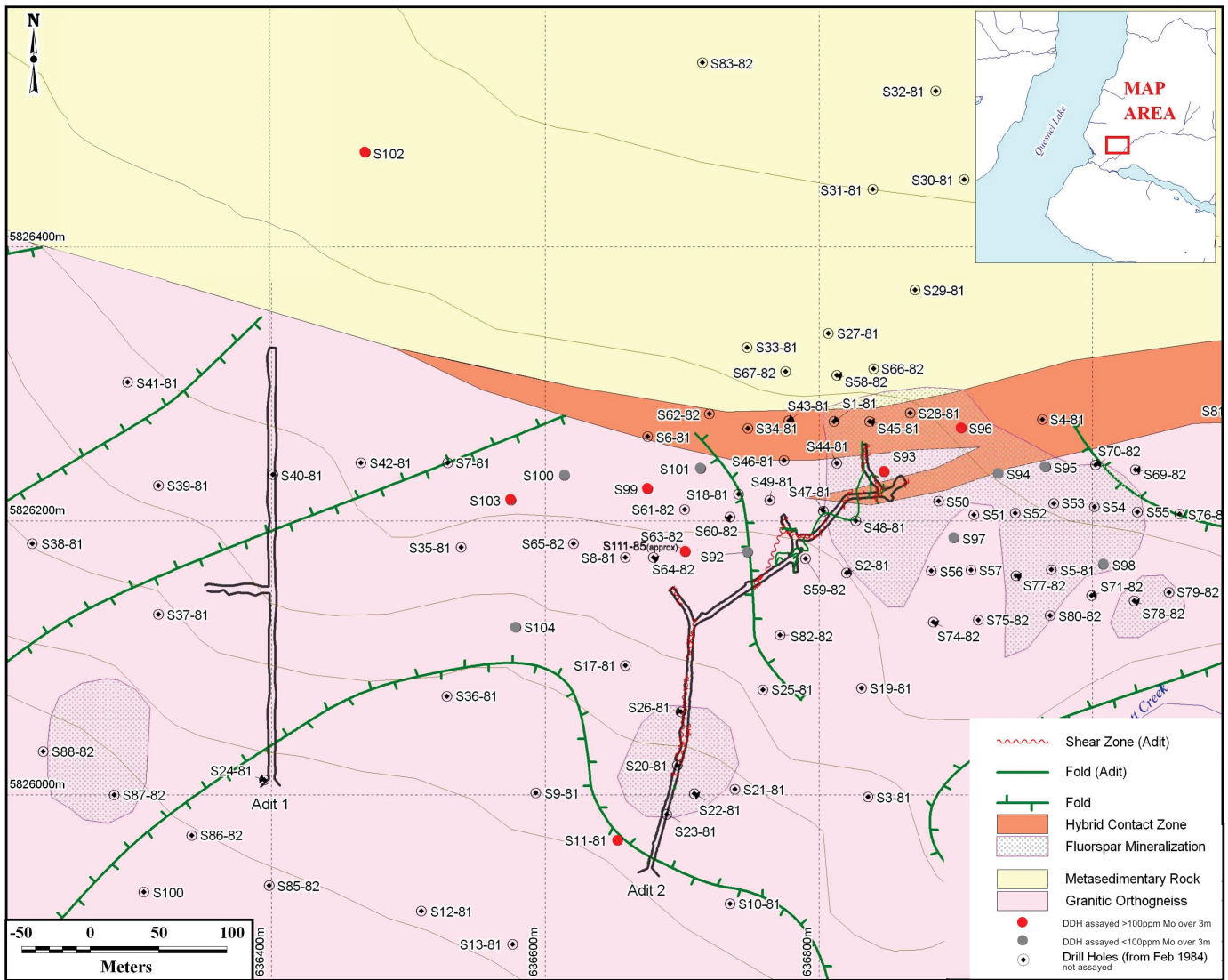


Fig. 2. Property map with adits and drill hole locations with Mo data. Courtesy of Freeport Resources Inc. (UTM Zone 10).

of Adit 2 (Fig. 3) and archived indoors at the British Columbia Geological Survey rock storage facility (designated Eaglet Adit 2, August 1984, East Drift mineral zone, Fig. 3).

Four samples collected from Adit 2 were submitted to the AIRIE program, Colorado State University for Re-Os isotopic determination of molybdenite. One sample contained molybdenite flakes in a quartz vein from a feldspathic gneiss that displayed incipient hydrothermal alteration, spotty rusty patches of iron oxide, veinlets of quartz with molybdenite, fluorite, and celestite (QLA 4; MD-1040). A second set of samples from the British Columbia Geological Survey archive collection were submitted for additional tests (Eaglet 0-1, MD-1311; and Eaglet 4, MD1312). The sample Eaglet 0-1 has molybdenite crystals in fluorite-celestite-quartz gangue and sample Eaglet 4 has molybdenite crystals in fluorite-calcite-celestite gangue with grains of siderite.

5.1. Re-Os methods

Re and Os isotopic measurements were obtained using negative thermal ionization mass spectrometry (NTIMS). Molybdenite separates were extracted from selected samples (Fig. 4) using a small hand-held drill. Molybdenite separates were 80-100% pure; sample weights ranged from 20-52 milligrams. Re-Os data were acquired using a Carius tube dissolution and a double Os spike; all samples were optimally spiked. All samples had less than 28 ppt common Os, of negligible consequence for the age calculation. Data are blank corrected, and corrected for Os isotope fractionation, and common Os. For MD-1040, blanks are Re=2.55 ±0.04 pg, Os=0.44 ±0.01 pg with $^{187}\text{Os}/^{188}\text{Os}=0.931 \pm 0.016$. For MD-1311 and MD-1312, blanks are Re=7.85 ±1.48 pg, Os=1.86 ±0.03 pg with $^{187}\text{Os}/^{188}\text{Os}=0.322 \pm 0.010$.

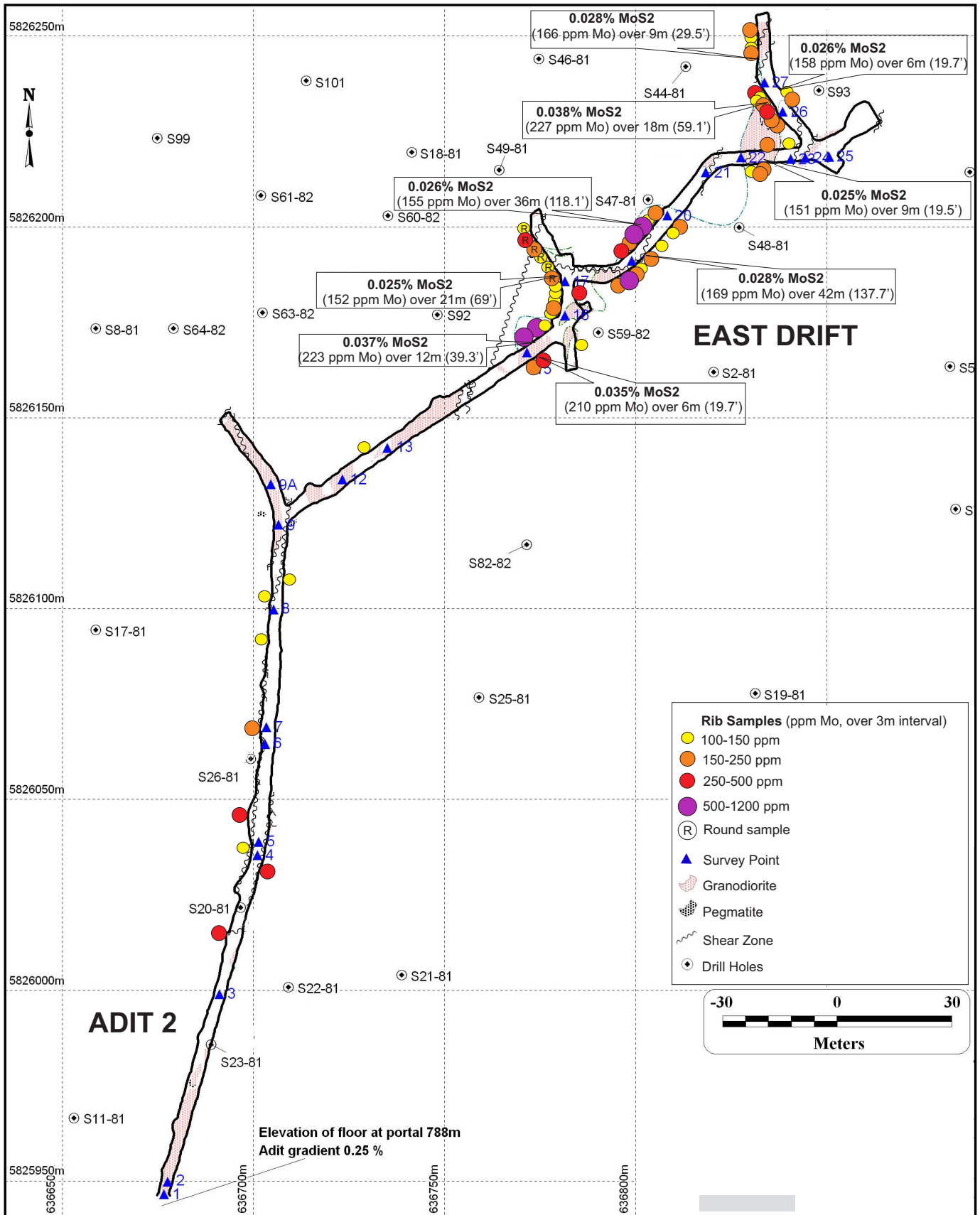


Fig. 3. Adit 2 with Mo results and East Drift mineralized zone (sample location). Courtesy of Freeport Resources Inc. (UTM Zone 10).

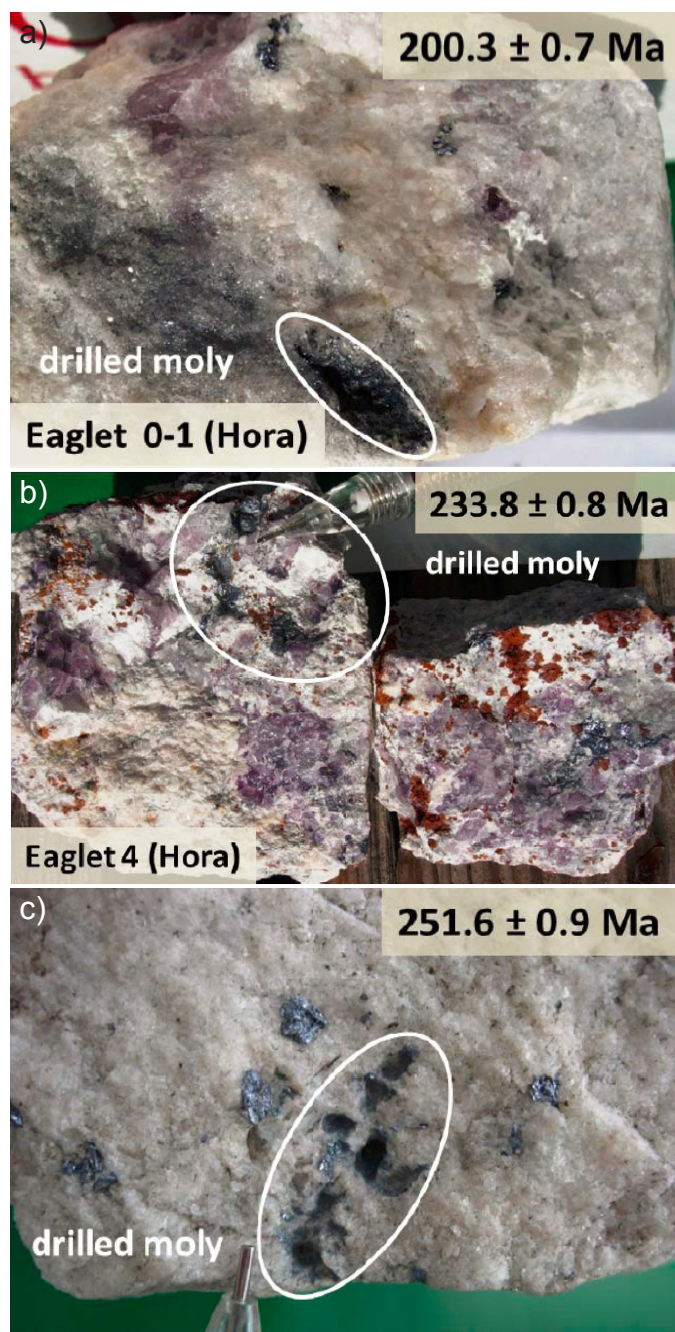


Fig. 4. Samples for Re-Os dating. **a)** MD-1311, molybdenite as small flakes in thin fluorite veinlets intersecting fluorite QL-1, spatially associated with celestite and quartz. **b)** MD-1312, molybdenite in thin fluorite veinlet in fluorite QLA-1, associated with celestite and siderite crystals. **c)** MD-1040, molybdenite in quartz vein from boulder, with celestite and fluorite QL-1 breccia veining.

5.2. Re-Os results

Re-Os data from the three Eaglet molybdenite samples from Adit 2 yielded three different model ages spanning 50 million years: 200.3 ± 0.7 Ma, 233.8 ± 0.8 Ma, and 251.6 ± 0.9 Ma (Table 1). The first sample is molybdenite in a quartz vein, whereas the other two are fissures in fluorite QL-1 and QLA-1. This type of age span is unexpected in a single deposit

and further work is warranted to assist interpreting the three disparate age results. Significant differences in molybdenite Re content from the same deposit are uncommon, but are known from other locations (Lawley and Selby, 2012) and do not affect the Re-Os results. Such differences may also reflect two polymorphose forms of molybdenite: 3R rhombohedral type, which usually carries higher Re with other impurities; and 2H hexagonal type, which is generally relatively pure (Newberry, 1979a, b). The XRD of the Eaglet molybdenite laboratory-scale concentrate sample tested in 2006 contained 33% of 3R and 22% of 2H types (Hora et al., 2008).

6. Sulphur isotope analyses

The analytical method used in this study is identical to that described in Hora et al. (2010). The initial sulphur isotope study of Hora et al. (2010) concentrated on celestite (five samples) with only two sulphide samples analyzed. Here we report eight additional $\delta^{34}\text{S}$ analyses of sulphide minerals from various mineral assemblages, including two pyrite-molybdenite pairs, i.e., minerals separated from the same samples (Table 2). The samples used for the Re-Os study were analyzed for sulphur isotopes as well.

Molybdenite in both sample sets demonstrates sulphur isotope homogeneity: $\delta^{34}\text{S}$ values fall in a narrow range between -3.93 and -5.04‰ , with variability slightly exceeding 1%. This suggests deposition of molybdenite within a single mineralization process or singular source of sulphur. Pyrite $\delta^{34}\text{S}$ values range more widely, from -4.84 to $+2.42\text{‰}$. The analyzed mineral pair pyrite-molybdenite are not in isotopic equilibrium, indicating most probably that they did not crystallize from the same hydrothermal fluid. Celestite $\delta^{34}\text{S}$ also has a higher variability, between $+6.00$ and $+12.91$. Sulphur in galena is much heavier than the other sulphides, perhaps indicating a source through reduction of sulphate (i.e., celestite) sulphur, which has a similarly heavy isotopic composition.

7. Fluid inclusions in fluorite

Fluorite is plentiful in drill core and adit dump piles, providing abundant material for fluid inclusion study. Several different colours, grain sizes, and textures of fluorite are obvious and commonly occur together in hand samples. As described by Hora et al. (2008) dark purple fluorite is the oldest phase (Fluorite QLA-11). Next to form were varieties of light purple and light green to almost colourless fluorite in randomly distributed aggregates and veinlets (Fluorite QL-1). Last to form were intergrowths of medium purple, sugary aggregates together with calcite (Fluorite QLA-1). Locally altered siderite is the final phase. Samples of all three macroscopically distinct types of Eaglet fluorite were selected for fluid inclusion study.

7.1. Methods

Microthermometric investigations of fluid inclusions were done at the Czech Geological Survey in Prague using a CHAIXMECA heating and freezing stage operating from -180 to $+500^\circ\text{C}$ (Poty et al., 1976). The accuracy of temperature

Table 1. Re-Os data for molybdenite from the Eaglet F-Mo deposit.

AIRIE Run #	Sample Name	Re, ppm	Re err, abs (ppm)	¹⁸⁷ Os, ppb	¹⁸⁷ Os err, abs (ppb)	Age, Ma
MD-1040	#QLA-4	81.55	0.08	215.3	0.2	251.6 ±0.9
MD-1311	#0-1	5.641	0.009	11.86	0.01	200.3 ±0.7
MD-1312	#4	2.802	0.004	6.873	0.006	233.8 ±0.8

Molybdenite separates are 80-100% pure; dilution is silicate which does not affect Re-Os age calculation; sample weights ranged from 20 to 52 milligrams.

Re-Os analyses by NTIMS using a Carius tube dissolution and a double Os spike; all samples were optimally spiked.

All samples had less than 28 ppt common Os, negligible to the age calculation.

Data are blank corrected, and corrected for Os isotope fractionation, and common Os.

For MD-1040, blanks are Re = 2.55 ±0.04 pg, Os = 0.44 ±0.01 pg with ¹⁸⁷Os/¹⁸⁸Os = 0.931 ±0.016.

For MD-1311 and MD-1312, blanks are Re = 7.85 ±1.48 pg, Os = 1.86 ±0.03 pg with ¹⁸⁷Os/¹⁸⁸Os = 0.322 ±0.010.

Table 2. Sulphur isotope data on the celestite and sulphide minerals of the Eaglet Property. All δ³⁴S values are reported relative to CDT international standard. Overall analytical uncertainty is ±0.2‰.

Sample No.	Mineralogy	δ ³⁴ S celestite	δ ³⁴ S sulphide	Re-Os age of molybdenite, Ma
Hora et al. (2010)				
QL A-1	celestite, fluorite, quartz	+6.00		
QL A-2	celestite, quartz, fluorite	+7.06		
QL A-3	quartz, celestite, fluorite, feldspar	+12.91		
QLA-4, MD -1040	celestite, quartz, fluorite, molybdenite	+7.12	molybdenite -4.81	251.6 ±0.9
QL A-5	celestite, fluorite, quartz, feldspar	+6.87		
QL C-1	calcite, celestite, pyrite	+9.86	pyrite: -4.84	
Present study				
MD-1311 0-1	molybdenite with celestite, fluorite, quartz		molybdenite -4.34	200.3 ±0.7
0-2	molybdenite with celestite and fluorite		molybdenite - 5.04	
0-3	pyrite, close to molybdenite 0-2, in celestite and fluorite		pyrite +0.99	
MD- 1312 4	molybdenite, close to pyrite 4, in celestite and fluorite with siderite crystals		molybdenite -3.93	233.8 ±0.8
12	pyrite, close to molybdenite 4 in celestite and fluorite with siderite crystals		pyrite -2.52	
14	pyrite intergrown with fluorite and molybdenite		pyrite +2.42	
16	pyrite, pure in fluorite and celestite		pyrite -3.03	
	galena, pure in fluorite, celestite and calcite		galena +12.07	

measurements is ±0.2°C at temperatures below 0°C and ±3°C at temperatures up to 400°C. The inclusions were classified according to Roedder's (1984) criteria for primary or secondary origins. Salinity (as wt.% NaCl equiv.) was calculated using the equations of Bodnar and Vityk (1995); the composition of the salt systems used the method described in Borisenko (1977).

V-T-X features of H₂O-CO₂ or H₂O-CH₄ inclusions were estimated according to Bakker and Diamond (2000) and Kerkhof and Thiery (2001). The density of CO₂ was calculated by the computer program FLUIDS (Bakker, 2003).

The fluid inclusion investigation began with characterizing fluid inclusion populations, also known as fluid inclusion

assemblages (FIAs). Petrographic description of fluid inclusions included the distribution of inclusions, their size, shape, liquid to vapour ratio, and their composition. Where fluid inclusion assemblages (FIAs) have uniform characteristics and occupy the same area of the sample, they are considered to have been trapped from the same hydrothermal fluid. Goldstein and Reynolds (1994) and Goldstein (2001) used the term 'fluid inclusion assemblages' as "the most finely discriminated, petrographically associated, group of inclusions".

The following phase transitions were measured in the inclusions.

- TmCO₂ - temperature of melting of solid CO₂
- TmclatCO₂ - temperature of melting of clathrate of CO₂
- ThCO₂ - temperature of homogenization of CO₂
- Tmice - temperature of melting of the last ice crystal
- Th - bulk homogenization temperature
- ThCH₄ - temperature of homogenization of CH₄
- LVR=L/(L+V) - liquid to vapour ratio

7.2. Results

7.2.1. Fluorite QLA-11

This sample is of dark purple fluorite considered the oldest variety in the Eaglet deposit (Hora et al., 2008). Primary inclusions in 3D distribution were found in the well-preserved parts of fluorite crystals and lack extensive trails of secondary inclusions. The inclusions measured have various shapes, range in long dimension from 5 to 80 μm, (Figs. 5 a, b) and have various compositions and numbers of contained phases.

H₂O, CO₂, or a mixture of these phases are common. H₂O inclusions have mostly consistent LVR=0.9, and are up to 20 μm in diameter. Tmice=-0.2 to -0.6°C, corresponding to salinities of an aqueous solution between 0.4 and 1.1 wt.% NaCl equivalent. Homogenization temperatures were measured only in inclusions with LVR=0.9, and ranged from 126 to 142°C.

H₂O-CO₂ inclusions are oval or fill space of crystal shape, up to 60 μm in diameter, and have LVR=0.4 to 0.7. TmCO₂ were measured between -56.3 and -57.5°C, which indicates very small amounts of CH₄ or N₂ in the vapour phase. TmclatCO₂=8.5 to 9.5°C, equal to the salinity of an aqueous solution from 1 to 3 wt.% NaCl equivalent. CO₂ homogenized to liquid at a temperature from 6.2 to 22.6°C. The density of CO₂=0.750-0.890 g/cm³. Homogenization temperatures were not observed because the inclusions consistently decrepitated, at about 230°C, before homogenization was achieved.

Several H₂O-CO₂ inclusions contain a small crystalline solid phase. Because the same isolated crystals can be found in solid fluorite, we believe that these crystals are not 'daughter crystals', i.e., crystallized from an oversaturated solution. Crystals are too small to identify (Fig. 5 b).

All inclusion types are observed together within one FIA indicating that they are contemporaneous. However, the inclusions can display variable composition, variable LVR, but a relatively narrow range of ThCO₂. Criteria supporting either a homogeneous or heterogeneous environment of inclusion trapping are ambiguous (Touret, 2001; Touret and Frezzotti,

2003). Measurements from pseudosecondary inclusions (see below) suggest that at least some of the H₂O-CO₂-rich inclusions were trapped in a homogeneous environment where H₂O-rich and CO₂-rich fluid phases were miscible (i.e., a single phase fluid that subsequently unmixed into immiscible CO₂ and H₂O phases; Fig. 5c).

A FIA containing H₂O-CO₂-rich fluid was found along short trails and are probably of pseudosecondary origin. These inclusions have a negative crystal shape and relatively consistent LVR=0.7. TmCO₂=-56.5°C, indicating pure CO₂ content in the vapour phase, TmclatCO₂=9.0 to 9.5°C, corresponding to the salinity of an aqueous solution between 1 and 2 wt.% NaCl equiv. The values of ThCO₂ (to liquid) ranged between 18.9 and 23.8°C, and the density of CO₂ was from 0.726 to 0.790 g/cm³. The bulk homogenization temperature ranged between 284 and 288°C.

An FIA with consistent LVR, ThCO₂ and Th within the narrow range can be considered as trapped in a homogeneous environment, where H₂O-rich and CO₂-rich phases are miscible. In such cases, bulk Th values are equal to the lowest temperatures of trapping of the inclusions (Fig. 5d). The minimum trapping pressure, constrained by temperature and composition, is about 2.1 to 2.6 Kb.

7.2.2. Fluorite QL-1

This sample represents the most abundant fluorite in the Eaglet deposit. It is usually massive and coarse grained, of lighter colours (purple or greenish to colourless). Primary H₂O-CO₂ inclusions were found along two distinct growth zones. The inclusions are oval to irregular shape, up to 40 μm in diameter (Fig. 5e), and have variable LVR. TmCO₂=-56.8 to -57.3°C, that indicate inclusions contain almost pure CO₂; Tmclat CO₂=8.7 to 9.2°C, corresponds to salinities between 1 and 3.5 wt.% NaCl equiv. CO₂ homogenized to liquid at temperatures from 6.5 to 8.5°C; the density of CO₂ was 0.874 to 0.887 g/cm³. Th values were not determined because the inclusions decrepitated before homogenization was attained.

7.2.3. Fluorite QLA-1

This fluorite is a later phase of intergrown medium purple fluorite, with calcite and highly altered siderite turned into rusty iron oxide. The fluorite contains primary oval inclusions up to 80 μm across (Fig. 5f), and variable LVR. This FIA is H₂O-rich. In some vapour-rich inclusions (LVR=0.1) methane was identified.

Homogenization temperatures of these H₂O-rich inclusions were measured for inclusions with LVR=0.8 to 0.9. Th values ranged from 108 to 159°C. Tmice was between -0.1 and -0.7°C, corresponding to salinities of 0.2 to 1.2 wt.% NaCl equivalent. CH₄ was identified only in several vapour-rich inclusions. CH₄ homogenized to liquid at temperature -85.6°C; it corresponds to a density of CH₄=0.217 g/cm³. H₂O and H₂O-CH₄ inclusions were probably trapped under conditions where the phases were immiscible.

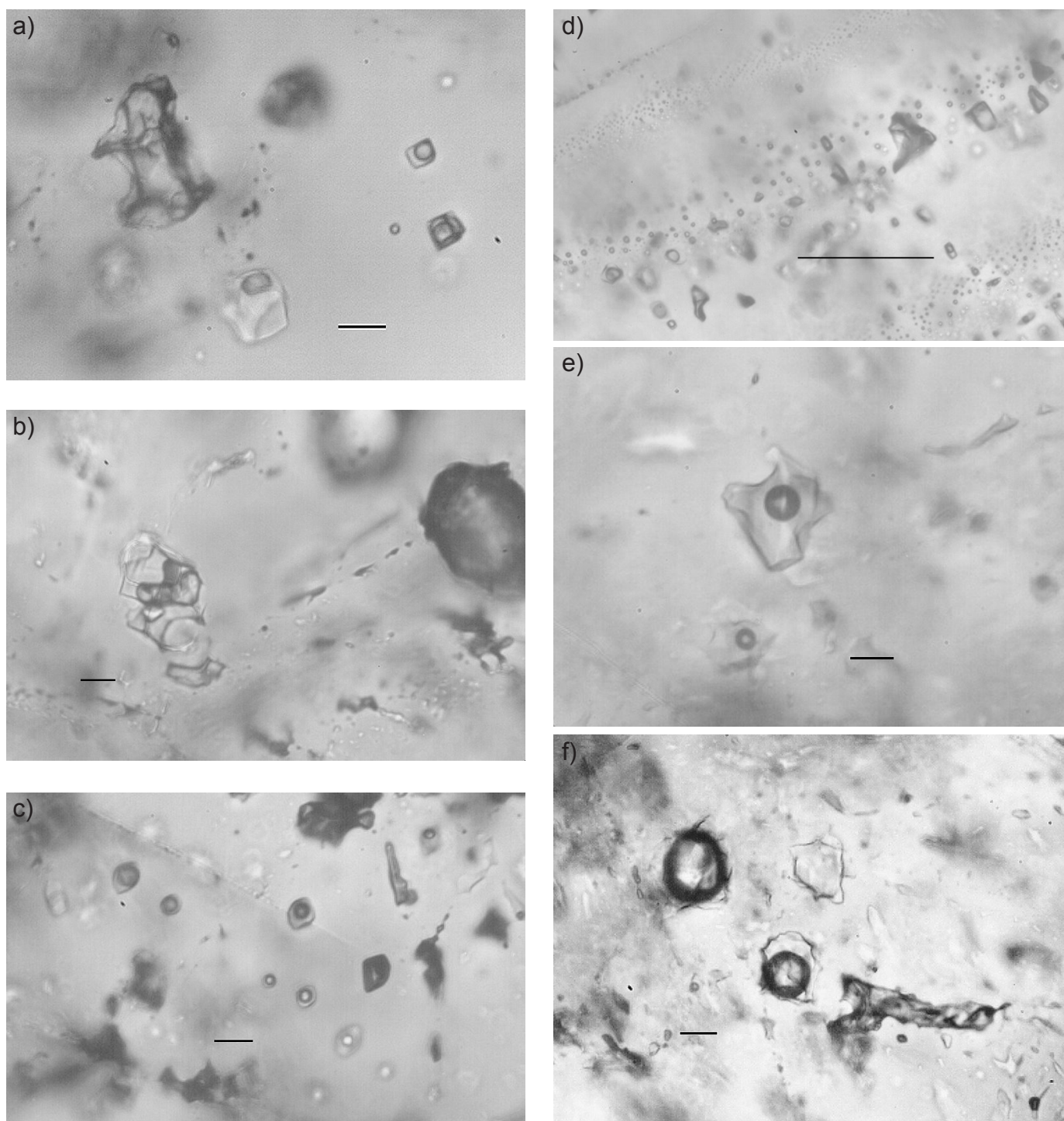


Fig. 5. Fluid inclusions. **a)** QLA-11 primary H₂O-CO₂ inclusions (scale 10µm). **b)** QLA-11 primary H₂O-CO₂ inclusions containing crystalline solid phase (scale 10µm). **c)** QLA-11 primary-secondary inclusions of H₂O-CO₂ type, consistent LVR (scale 10µm). **d)** QLA-11 secondary H₂O-CO₂ inclusions (scale 100µm). **e)** QLA-1 primary H₂O inclusions (scale 10µm). **f)** V>L primary H₂O-CH₄ inclusions (scale 10µm).

8. Discussion

Widespread distribution of molybdenite in reanalyzed drill core pulps and Adit 2 samples suggest that Mo could be a potential co-product should the deposit ever be mined. Re-Os molybdenite model ages appear to record molybdenite mineralization at 251.6 ±0.9 Ma, 233.8 ±0.8 Ma and

200.3 ±0.7 Ma, spanning 50 million years. To our knowledge, such long-term episodicity is unknown in porphyry deposit settings. Especially surprising is that all three samples come from the same highly mineralized zone intersected in Adit 2 and all three samples plot in a narrow range of molybdenite δ³⁴S values, suggesting a uniform sulphur source.

With respect to sulphur sources, the data can be interpreted in two ways. Either the sulphate (celestite) oxidized sulphur and reduced sulphur were derived (recycled) from two different crustal sulphur sources, or the observed pattern resulted from a high-temperature isotope exchange between reduced and oxidized sulphur in the hydrothermal fluids (Ohmoto and Lasaga, 1982). With respect to sulphur isotope homogeneity of the molybdenite the first possibility is more probable. In molybdenite, the sulphur isotope data are very close whereas those in celestite vary more widely.

Macroscopic observations and limited microprobe data suggest that molybdenite growth was independent of celestite, which also supports independent sulphur sources and/or different fluid histories leading to growth of these two minerals (Hora et al., 2008). Some molybdenite may have recrystallized and thus reset the Re-Os geochronometer while retaining the same $\delta^{34}\text{S}$ composition (Suzuki et al., 2001). This process requires Re and Os decoupling and Os mobility within single molybdenite crystals (Stein et al., 2003; Košler et al., 2003; Aleinikoff et al., 2012). Further work will be required to test this possibility.

Complexity in mineralogy and chemical composition makes the Eaglet deposit difficult to assign to a specific mineral deposit type. Nevertheless, the style of mineralization at Eaglet is probably not unique. In a similar pericratonic location, some 150 km southeasterly from Eaglet, is the Rexspar fluorite deposit (also known as Birch Island; MINFILE 082M 007, 021, 022, 034 and 043). Sheared mineralized breccias reportedly contain a similar suite of associated minerals: molybdenite, celestite, strontianite, chalcopyrite, galena, niobian ilmenorutile, and a variety of uranium and thorium minerals in a pervasive potassium alteration halo (Pell, 1992). Unfortunately, Re-Os and sulphur isotope data are lacking and the mineralization at Rexspar is not sufficiently characterized to permit more detailed comparison.

9. Conclusions

Analytical work presented here further characterizes mineralization at the Eaglet property. Sulphur isotope data support work reported previously that indicated distinct and multiple phases of different types of mineralization, including Nb, REE and celestite. Most important is the peculiarity of three different Re-Os ages for molybdenite with consistent sulphur isotopic compositions suggesting derivation from a homogeneous sulphur isotope reservoir. In contrast, pyrite and celestite have much higher $\delta^{34}\text{S}$ variability. The significance of the multiple Re-Os ages remains unresolved and requires additional study.

The three distinct types of fluorite sampled from the Eaglet deposit have different FIA chemistries. Of the three samples, two contain FIAs with differing $\text{H}_2\text{O}-\text{CO}_2$ mixtures, or almost a pure CO_2 in some instances. The oldest, dark purple fluorite contained inclusions of a solid crystalline phase conspicuously absent in most common, pale coloured fluorite type. Fluid inclusions in a sample of youngest fluorite phase contained

significant methane component (CH_4).

A multiphase mineralizing history is suggested by the Re-Os geochronology; three different populations of fluorite with distinct fluid inclusion assemblage compositions; hydrothermal overprinting of early phase Nb-Th-Ti-REE mineralization (Hora et al., 2010), and an overall multi-stage stockwork character, with late emplacement of celestite. The economic potential of the Eaglet property is not established.

Acknowledgments

In memoriam of our colleague Edvin Pivec, who helped to coordinate several phases of the Eaglet property research. Due to his untimely death he could not participate in concluding work on the project. Initial support of this work was partly funded by the Beetle Impacted Zone project under the auspices of the British Columbia Geological Survey. Continued interest and support by Mitch Mihalynuk and Freeport Resources Inc. are appreciated. Review of an initial draft by Dave Lefebure and Mitch Mihalynuk significantly improved the final text. Participation of K. Žák was possible thanks to the support by the RVO67985831 program. I. Jačková prepared the samples and operated the mass spectrometer to obtain the sulphur isotope data. Kirk Hancock helped prepare the final draft. The final text was improved by reviewers L. Ootes and S.M. Rowins.

References cited

- Aleinikoff, J.N., Creaser, R.A., and Lowers, H.A., 2012. Multiple age components in individual molybdenite grains. *Chemical Geology*, 300-301, 55-60.
- Bakker, R.J., 2003. Package FLUIDS 1. Computer programs for analysis of fluid inclusion data and for modelling bulk fluid properties. *Chemical Geology*, 194, 3-23.
- Bakker, R.J., and Diamond, L.W., 2000. Determination of the composition and molar volume of $\text{H}_2\text{O}-\text{CO}_2$ fluid inclusions by microthermometry. *Geochimica et Cosmochimica Acta*, 64, 1753-1764.
- Ball, C.W., and Boggaram, G., 1985. Geological investigation of the Eaglet fluorspar deposit. *Mining Magazine*, 30, 506-509.
- Bodnar, R.J., and Vityk, M.O., 1995. Interpretation of microthermometric data for $\text{H}_2\text{O}-\text{NaCl}$ fluid inclusions. In: De Vivo, B., Frezzotti, M.L., (Eds.), *Fluid Inclusions in Minerals: Methods and Applications*. Short course of the working group Inclusions in Minerals. Blacksburg, VA, Virginia Polytechnic Institute, pp. 117-130.
- Borisenko, A.S., 1977. Cryotechnic methods for the determination of fluid inclusions salts in minerals. *Geologia i Geofizika*, 8, 16-27. (in Russian).
- Ferri, F., and Schiarizza, P., 2006. Reinterpretation of the Snowshoe Group stratigraphy across a southwest-verging nappe structure and its implications for regional correlations within the Kootenay terrane. In: Colpron, M., and Nelson, J.L., (Eds.), *Paleozoic Evolution and Metallogeny of Pericratonic Terranes at the Ancient Pacific Margin of North America*, Canadian and Alaskan Cordillera. Geological Association of Canada Special Paper 45, pp. 415-432.
- Ferri, F., Höy, T., and Friedman, R.M., 1999. Description, U-Pb age and tectonic setting of the Quesnel Lake gneiss, east-central British Columbia. In: *Geological Fieldwork 1998*, British Columbia Ministry of Energy and Mines, British Columbia Geological Survey Paper 1999-1, pp. 69-80.
- Goldstein, R.H., 2001. Fluid inclusions in sedimentary and

- diagenetic systems. *Lithos*, 55, 159-192.
- Goldstein, R.H., and Reynolds T.J., 1994. Systematics of fluid inclusions in diagenetic minerals. *SEPM Short Course*, 31, Tulsa, 199 p.
- Hora, Z.D., 2005. Analytical report on new assay data from 1980-1984 drill core samples, Q claims Cariboo Mining Division. British Columbia Ministry of Energy, Mines and Petroleum Resources, Assessment Report 27823.
- Hora, Z.D., Langrová A., and Pivec, E., 2008. Eaglet property revisited: Fluorite-molybdenite porphyry-like hydrothermal system, east-central British Columbia (NTS 093A/10W). In: *Geological Fieldwork 2007*, British Columbia Ministry of Energy, Mines and Petroleum Resources, British Columbia Geological Survey Paper 2008-1, pp. 17-30.
- Hora, Z.D., Langrová A., Pivec, E., and Žák, K., 2010. Niobium-thorium-strontium-rare earth element mineralogy and preliminary sulphur isotope geochemistry of the Eaglet property, east-central British Columbia (NTS 093A/10W). In: *Geological Fieldwork 2009*, British Columbia Ministry of Forests, Mines and Lands, British Columbia Geological Survey Paper 2010-1, pp. 93-96.
- Kerkhof van den, A., and Thiéry, R., 2001. Carbonic inclusions. *Lithos*, 55, 49-68.
- Košler, J., Simonetti, A., and Sylvester, P.J., 2003. Laser-ablation ICP-MS measurements of Re/Os in molybdenite and implications for Re-Os geochronology. *Canadian Mineralogist*, 41, 307-320.
- Lawley, C.J.M., and Selby, D., 2012. Re-Os geochronology of quartz-enclosed ultrafine molybdenite: implications for ore geochronology. *Economic Geology*, 107, 1499-1505.
- McCammon, J.W., 1965. Fluorite: Eaglet group. British Columbia Ministry of Mines, Annual Report 1965, 263-264.
- Newberry, R.J., 1979a. Polytypism in molybdenite (I): a non-equilibrium impurity-induced phenomenon. *American Mineralogist*, 64, 758-767.
- Newberry, R.J., 1979b. Polytypism in molybdenite (II): relationship between polytypism, ore deposition/alteration stages and rhenium contents. *American Mineralogist*, 64, 768-775.
- Ohmoto, H., and Lasaga, A.C., 1982. Kinetics of reactions between aqueous sulphates and sulphides in hydrothermal systems. *Geochimica et Cosmochimica Acta*, 46, 1727-1745.
- Pell, J., 1992. Fluorspar and fluorine in British Columbia. British Columbia Ministry of Energy, Mines and Petroleum Resources, British Columbia Geological Survey Open File 1992-16, 82 p.
- Poty, B., Leroy, J., and Jachimowicz, L., 1976. A new device for measuring the temperature under the microscope: the Chaixmeca microthermometry apparatus. *Bulletin de la Societe Francaise de Mineralogie et de Cristallographie*, 99, 182-186.
- Roedder, E., 1984. Fluid inclusions. *Reviews in Mineralogy*. Mineralogical Society of America, 644 p.
- Stein, H.J., Markey, R.J., Morgan, J.W., Hannah, J.L., and Schersten A., 2001. The remarkable Re-Os chronometer in molybdenite: how and why it works. *Terra Nova*, 13, 479-486.
- Stein, H.J., Schersten, A., Hannah, J., and Markey, R., 2003. Sub-grain scale decoupling Re and ¹⁸⁷Os and assessment of laser ablation ICP-MS spot dating in molybdenite. *Geochimica et Cosmochimica Acta*, 67, 3673-3686.
- Suzuki, K., Feely, M., and O'Reilly C., 2001. Disturbance of the Re-Os chronometer of molybdenite from the late-Caledonian Galway Granite, Ireland, by hydrothermal fluid circulation. *Geochemical Journal*, 35, 29-35.
- Touret, J.L.R., 2001. Fluids in metamorphic rocks. *Lithos*, 55, 1-25.
- Touret, J.L.R., and Frezzotti, M.L., 2003. Fluid inclusions in high pressure and ultrahigh pressure metamorphic rocks. In: Carswell, D.A., and Compagnoni, R., (Eds.), *Ultrahigh-Pressure Metamorphism*, E.M.U. Notes in Mineralogy, 5, pp. 467-487.